MBoC | ARTICLE

Loss of Grp170 results in catastrophic disruption of endoplasmic reticulum function

Melissa J. Mann[a], Chris Melendez-Suchi[a], Hannah E. Vorndran[b], Maria Sukhoplyasova[b], Ashley R. Flory[a], Mary Carson Irvine[a], Anuradha R. Iyer[b], Christopher J. Guerriero[b], Jeffrey L. Brodsky[a,b], Linda M. Hendershot[a,†], and Teresa M. Buck[a,b,†,*]

[a]Department of Tumor Cell Biology, St. Jude Children's Research Hospital, Memphis, TN 30105; [b]Department of Biological Sciences, University of Pittsburgh, Pittsburgh, PA 15260

ABSTRACT **GRP170 (*Hyou1*) is required for mouse embryonic development, and its ablation in kidney nephrons leads to renal failure. Unlike most chaperones, GRP170 is the lone member of its chaperone family in the ER lumen. However, the cellular requirement for GRP170, which both binds nonnative proteins and acts as nucleotide exchange factor for BiP, is poorly understood. Here, we report on the isolation of mouse embryonic fibroblasts obtained from mice in which LoxP sites were engineered in the *Hyou1* loci (*Hyou1*$^{LoxP/LoxP}$). A doxycycline-regulated Cre recombinase was stably introduced into these cells. Induction of Cre resulted in depletion of Grp170 protein which culminated in cell death. As Grp170 levels fell we observed a portion of BiP fractionating with insoluble material, increased binding of BiP to a client with a concomitant reduction in its turnover, and reduced solubility of an aggregation-prone BiP substrate. Consistent with disrupted BiP functions, we observed reactivation of BiP and induction of the unfolded protein response (UPR) in futile attempts to provide compensatory increases in ER chaperones and folding enzymes. Together, these results provide insights into the cellular consequences of controlled Grp170 loss and provide hypotheses as to why mutations in the *Hyou1* locus are linked to human disease.**

Monitoring Editor
Guillaume Thibault
Nanyang Technological University

Received: Jan 8, 2024
Revised: Feb 20, 2024
Accepted: Feb 29, 2024

Challenge

SIGNIFICANCE STATEMENT

- GRP170 is an endoplasmic reticulum (ER) localized molecular chaperone that is associated with both protein folding and quality control. How loss of GRP170 affects cellular homeostasis is unknown.
- The authors used an inducible Grp170 KO cell model system to determine that loss of Grp170 results in disruption of proteostasis, induction of the unfolded protein response (UPR) and loss of cell viability.
- These findings characterize an essential role for GRP170 in cellular physiology and will provide insight as to the pathology of GRP170 mutants in human disease.

This article was published online ahead of print in MBoC in Press (http://www.molbiolcell.org/cgi/doi/10.1091/mbc.E24-01-0012) on March 6, 2024.

†Corresponding authors

*Address correspondence to: Teresa M. Buck (teb20@pitt.edu).

Abbreviations used: ERQC, endoplasmic reticulum quality control; Grp170, glucose regulated protein-170; BiP, binding protein; Grp94, glucose-regulated protein-94; Hsp70, heat shock protein-70; Hsp90, heat shock protein-90; ER, endoplasmic reticulum; NEF, nucleotide exchange factor; ERAD, endoplasmic reticulum associated degradation; UPR, unfolded protein response.

INTRODUCTION

Approximately one-third of the proteins encoded by the human genome will enter the endoplasmic reticulum (ER) co- or posttranslationally (Dancourt and Barlowe, 2010) where they will undergo a variety of modifications, fold, and assemble into their native form (Braakman and Bulleid, 2011; Phillips and Miller, 2021). This process is monitored by a dedicated ER quality control system (ERQC) that ensures only properly matured proteins are transported to the Golgi and to points further along the secretory pathway (Adams *et al.*, 2019; Pobre *et al.*, 2019; Hendershot *et al.*, 2023). To meet these demands, ERQC is comprised of a large complement of resident molecular chaperones, their cofactors, and two groups of folding

enzymes, which bind unfolded polypeptide chains as they enter the ER lumen. Together they protect vulnerable hydrophobic or aggregation prone regions on nascent proteins until they are buried upon folding and prevent the transport of immature intermediates. Equally important to the fidelity of the secretome is the need to identify proteins that fail to complete folding and/or assembly and target them for degradation by the proteasome (Vembar and Brodsky, 2008; Krshnan *et al.*, 2022; Christianson *et al.*, 2023). This ER-associated degradation (ERAD) pathway relies on some of the same chaperones and folding enzymes that assist protein folding and assembly in the ER to deliver misfolded proteins to a retrotranslocon complex for extraction to the cytosol (Wu and Rapoport, 2021). However, failure to match the demands of the biosynthetic load of the ER triggers the unfolded protein response (UPR) that strives to restore homeostasis, but if unsuccessful, prolonged UPR activation can result in cell death (Walter and Ron, 2011; Hetz *et al.*, 2020).

Many of the nascent proteins that enter the ER will ultimately reside in organelles of the secretory pathway, or they will be expressed at the cell surface or secreted into the extracellular space. This diverse polypeptide ensemble is modified by disulfide bonds and N-linked glycosylation, which serves in part to stabilize the polypeptide when transported to spaces without chaperones. Over 20 ER-resident protein disulfide isomerases (PDIs) assist in the formation, reduction, or isomerization of disulfide bonds (Appenzeller-Herzog and Ellgaard, 2008; Robinson and Bulleid, 2020), and two lectin chaperones and their cofactors assist in glycoprotein maturation (Molinari and Hebert, 2015). Disruption of individual members of these components of the ERQC machinery is largely tolerated due to redundancy among family members. Yet, in spite of the unique modifications to which proteins in the ER are subject, more general aspects of protein folding in the ER follow the same mechanisms that guide the transition of nascent polypeptide chains to their native conformations in the cytosol (Balchin *et al.*, 2016). In keeping with this view, the ER also possesses multiple members of both the cyclophilin and FKBP prolyl-peptidyl isomerase (PPIase) families, which catalyze the *cis-trans* isomerization of peptide bonds N-terminal to specific proline residues (Schiene-Fischer, 2015).

In contrast to the redundancy provided by the chaperone/folding families with multiple members, the mammalian ER possesses a single cognate of the Hsp70 (BiP/GRP78), Hsp90 (GRP94), and Hsp110 (GRP170) chaperone families. BiP, the first chaperone discovered in the ER, was identified through its association with unassembled immunoglobulin (Ig) heavy chains (Haas and Wabl, 1984; Bole *et al.*, 1986). BiP recognizes short hydrophobic polypeptide stretches on nascent proteins (Flynn *et al.*, 1991; Blond-Elguindi *et al.*, 1993) that are ultimately buried in the native state, providing its specificity for unfolded proteins. Genetic disruption of BiP in mice is embryonic lethal at day e3.5 (Luo *et al.*, 2006), and the AB5 subtilase cytotoxin kills cells by cleaving BiP between the client-binding domain and regulatory nucleotide-binding domain (Paton *et al.*, 2006), findings that reveal the essential nature of this chaperone. Although BiP is the only Hsp70 family member in the ER, it is assisted by one of eight DnaJ family cochaperones. Four of these, ERdj3-6, can bind a variety of clients and transfer them to BiP, which allows these chaperones to contribute to diverse and even opposing ER functions (Pobre *et al.*, 2019). At the cellular level, deletion of individual members of the Erdj family is tolerated and single knockout cells are viable (Amin-Wetzel *et al.*, 2017).

Like BiP, GRP94 – the lone Hsp90 family member in the ER – is required for mouse embryonic development, with null mice dying between day e6.5 – e7.5 (Wanderling *et al.*, 2007). Similar to the cytosolic Hsp90s, GRP94 has a more restricted clientele, which likely accounts for the essential nature of this gene in some tissues but not others. For instance, a mouse pre-B cell line was identified that lacks GRP94 (Randow and Seed, 2001), and embryonic stem cells can be isolated from a constitutive knockout mouse, which will differentiate into adipocytes, hepatocytes, and neurons, although not into myocytes (Wanderling *et al.*, 2007). Similarly, tissue-specific expression of Cre, which was used to delete the *GRP94*-encoding gene, is readily tolerated in the mammary gland (Zhu *et al.*, 2014), but Cre expression in myeloid precursors (Luo *et al.*, 2011), hepatocytes (Poirier *et al.*, 2015), or pancreatic β islet cells (Kim *et al.*, 2018) alters differentiation or adversely affects function.

GRP170, which belongs to the family of large Hsp70 proteins that includes cytosolic Hsp110, is the lone ER member of this chaperone family. GRP170 acts as a nucleotide exchange factor (NEF) for BiP to stimulate its release from clients (Steel *et al.*, 2004; Weitzmann *et al.*, 2006). In addition to its NEF activity, GRP170 acts as a molecular chaperone that binds aggregation-prone sequences in nonnative proteins (Park *et al.*, 2003; Behnke and Hendershot, 2014; Behnke *et al.*, 2016). GRP170 has also been shown to regulate the maturation of the trimeric epithelial sodium channel (ENaC) as it matures in the ER and participates in the ERAD of unassembled ENaC subunits (Buck *et al.*, 2013, 2017; Sukhoplyasova *et al.*, 2023). Attempts to produce Grp170 null mice were unsuccessful (Kitao *et al.*, 2001), revealing an essential role for this chaperone during mouse development, despite the presence of a structurally unrelated, second NEF in the ER lumen, Sil1 (Chung *et al.*, 2002). These data are consistent with unique functions of the two ER NEFs and are further supported by the identification of a human disease directly linked to SIL1 mutations (Anttonen *et al.*, 2005; Senderek *et al.*, 2005); mutations in the GRP170-encoding gene, *Hyou1*, were also recently linked to human disease (Kovacs *et al.*, 2002, Haapaniemi *et al.*, 2017). Additional support for the unique activities of the GRP170 and Sil1 NEFs was provided by the generation of a Cre-inducible nephron-specific mouse strain in which LoxP sites were engineered in the *Hyou1* loci (*Hyou1*$^{LoxP/LoxP}$). Regulated expression of Cre recombinase in kidney nephrons led to rapid excision of this gene, resulting in mice with hallmarks of renal cell injury and kidney disease (Porter *et al.*, 2022). Yet, the cellular and molecular mechanisms underlying renal cell damage remain ill-defined.

To this end, we created an experimentally tractable system to characterize the role of GRP170 in regulating various aspects of ER function and response to stress. Specifically, mouse embryonic fibroblasts (MEFs) were obtained from *Hyou1*$^{LoxP/LoxP}$ animals and transduced with a lentivirus encoding a doxycycline-regulated Cre recombinase. Single cell clones were isolated that rapidly and reproducibly resulted in complete excision of the *Hyou1* loci upon doxycycline treatment. Even though *Sil1* was induced, the depletion of murine Grp170 led to wide-spread disruption of BiP functions, collapse of ER homeostasis, and activation of the UPR, culminating in apoptotic cell death. These data further support unique activities of the two ER lumenal NEFs, highlight previously uncharacterized features of Grp170 function in the ER, and describe a tool to better define how Grp170 oversees ERQC.

RESULTS

Isolation of Hyou1$^{LoxP/LoxP}$ MEFs and creation of an inducible Cre construct

Fibroblasts were isolated from 12.5 d embryos generated from *Hyou1*$^{LoxP/LoxP}$ female mice that has been crossed with *Hyou1*$^{LoxP/LoxP}$ males, and cultured cells were transformed with SV40. In an attempt

to produce stable Grp170 null MEFs, the cells were transduced with lentivirus expressing GFP and Cre recombinase under control of a constitutive SV40 promoter (Qin *et al.*, 2010). However, two separate viral transductions with a multiplicity of infection (MOI) of two resulted in no GFP positive cells (unpublished data), suggesting that MEFs might be unable to tolerate loss of Grp170. Thus, a lentivirus backbone was engineered with a doxycycline-inducible Cre recombinase separated from mCherry with a P2A ribosome cleavage peptide (Supplemental Figure S1A). The construct was first tested in HEK293T cells, and after 2 d, GFP and mCherry expression were monitored by FACS. In the absence of doxycycline, GFP was readily detected with only a minor population of cells that also expressed mCherry (Supplemental Figure S1B), whereas doxycycline addition resulted in linear expression of mCherry corresponding to GFP levels. Cell lysates were then examined for Cre expression by western blotting, which revealed that mCherry fluorescence faithfully reported on Cre recombinase expression (Supplemental Figure S1C).

Continuous expression of Cre recombinase is selected against in Hyou$^{LoxP/LoxP}$ MEFs

We next introduced the Cre-modified lentivirus into *Hyou*$^{LoxP/LoxP}$ MEFs and sorted the cells to isolate a bulk culture of GFP$^+$ and mCherry$^-$ cells. Although this bulk culture was selected based on GFP expression, we observed a population of cells that were no longer GFP$^+$ as the sorted cells were expanded (Figure 1A, UT [untreated]). The cultured cells were then treated with doxycycline to induce Cre recombinase expression, and both GFP and mCherry fluorescence were monitored at various time points thereafter (Figure 1A). Cre recombinase induction and its effect on Grp170 expression were directly examined by RT-PCR and western blot (see below). After 2 d of doxycycline treatment, ~50% of the cells coexpressed both fluorescent proteins. However, several changes were observed over time. First, the population of cells expressing mCherry (and presumably Cre recombinase) dropped precipitously until they virtually vanished. Second, just over 50% of the cells at later time points expressed only GFP, indicating the cells in which mCherry was not induced by doxycycline had been positively selected. Third, the minor population of cells that did not express GFP at the beginning of the time course had expanded until they comprised 50% of the culture by d 11. This suggested that extinguishing Grp170 expression was toxic to MEFs.

In keeping with the pattern observed for mCherry expression, Cre mRNA and protein were readily observed after 2 d of doxycycline treatment. Cre expression was dramatically reduced by day 4 of doxycycline treatment and was undetectable thereafter (Figure 1, B and C). Correspondingly, after 2 d of treatment, *Grp170* mRNA and protein decreased to ~60 and ~80%, respectively, with similar levels on day 4. Because only ~50% of cells expressed mCherry/Cre, we surmised that Grp170 protein levels in the Cre positive cells were likely ~30–40% of that observed in untreated cells (UT) on these respective days. Consistent with the nearly complete loss of cells expressing mCherry/Cre from the bulk population, by day 7 *Grp170* transcript levels were the same as controls. We also monitored BiP levels because BiP shares clients with GRP170 (Behnke and Hendershot, 2014) and – as noted above – is the target of GRP170's nucleotide exchange activity (Steel *et al.*, 2004; Weitzmann *et al.*, 2006). The expression of BiP transcripts and protein increased as Grp170 levels declined and peaked on day 4. As Cre$^+$ cells disappeared and Grp170 levels normalized, BiP transcripts also returned to baseline, although BiP protein levels were slower to decline (Figure 1, B and C), likely due to its long half-life (Wang *et al.*, 2017).

Isolation of single cell Hyou$^{LoxP/LoxP}$ clones expressing inducible Cre recombinase

Because we were unable to isolate a bulk culture of Grp170 null MEFs, we next isolated single-cell clones in an effort to obtain cells with tight suppression of Cre recombinase in the absence of doxycycline, and to determine if complete ablation of Grp170 expression was possible with doxycycline treatment. To do so, we isolated the brightest ~15% of GFP$^+$ cells from the bulk culture and chose 88 single cell clones to expand and characterize. An aliquot of each clone was treated with doxycycline and examined for GFP and mCherry expression. Of these, only five clones were >90% positive for both GFP and mCherry (Table 1). These results were obtained despite each clone arising from a single cell, underscoring the enormous selective pressure against expressing Cre recombinase and thus eliminating Grp170 expression. Nevertheless, two of the isolated clones were >99% positive for both fluorescent proteins (clone A10 and E8) and were used for further analyses.

To begin to characterize the A10 and E8 clones, the kinetics and magnitude of doxycycline-induced Grp170 deletion were examined using two sets of primers that identified the intact gene and one set that detected the Cre-recombined, deleted gene (Supplemental Figure S2, A and B). Within 18 h the intact gene was no longer detected, suggesting that disruption of the Grp170-encoding alleles was complete. When the primer set that detected the gene deletion was used (i.e., F51 and R32), we observed an unexpected signal in the absence of doxycycline in both clones, although this signal increased over time with doxycycline treatment (Supplemental Figure S2B). This result was also observed in the other three clones with high inducible mCherry expression (unpublished data). To further characterize the unexpected evidence for rearrangement of the *Hyou1* gene in the absence of doxycycline, we performed fluorescence in situ hybridization (FISH) analysis on the A10 and E8 clones before and after doxycycline treatment. Both lines were polyploid, which is a consequence of SV40-transformation (Ray *et al.*, 1990). In the A10 clone, 98.5% of the cells had three copies of the region surrounding the *Hyou1* locus, as detected with a probe for the *Hyou1* telomeric flanking region (red signal), only two of which still contained the *Hyou1* gene (green signal) (Supplemental Figure S2C, untreated). The loss of *Hyou1* from the third copy explained the signal with the primer pair for a rearranged allele. In the E8 clone, 97% of the cells had four copies of this locus. Of these, 58% had one *Hyou1* allele deleted and 42% had two alleles deleted, thereby explaining the evidence for recombination in untreated cells shown in Supplemental Figure S2B. All the cells in both clones retained at least two copies of the *Hyou1* gene. After Cre recombinase induction with doxycycline, 200 cells were analyzed for each of the experimental groups, and the numbers of intact versus deleted genes was determined. Cells in which the *Hyou1* gene was intact had paired red-green signals, while loci that underwent programmed deletion had only the control flanking genomic region (i.e., red signal) present. We observed a complete loss of the green (*Hyou1*) signal in 100% of the cells that were counted in both clones, regardless of how many copies of the gene they possessed (Supplemental Figure S2C). This finding, coupled with our inability to amplify the two genomic sequences containing the LoxP sites, argues for complete disruption of the *Hyou1* gene upon Cre induction.

Grp170 is an essential protein

The levels of basal *Grp170* transcripts and protein in these two clones were compared with the nontransformed MEFs and to the SV40-transformed MEFs in which the doxycycline-inducible Cre system had not been introduced. The SV40-transformed MEFs

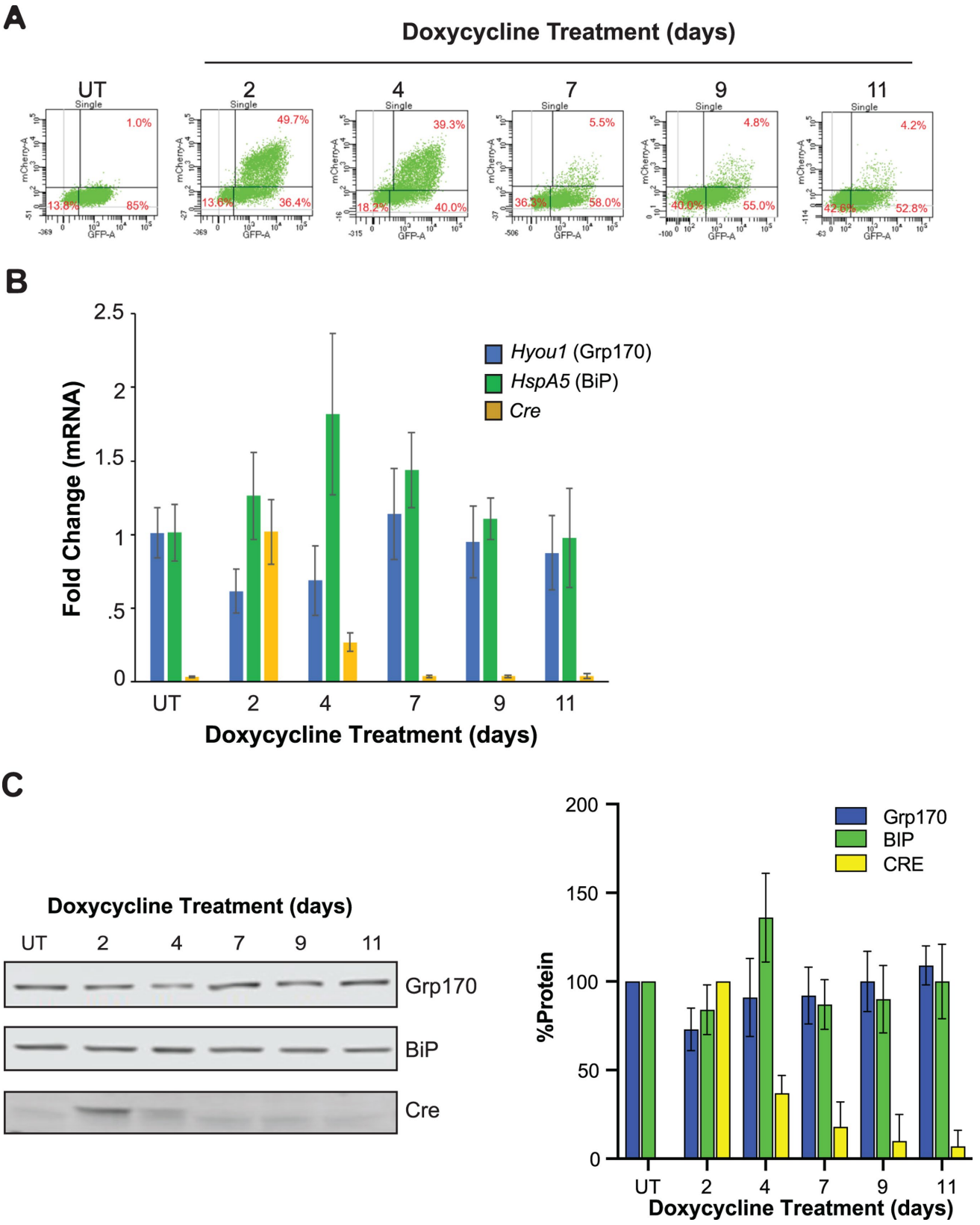

FIGURE 1: *Hyou1*$^{fl/fl}$ MEF cells expressing Cre recombinase are rapidly out-competed by cells that do not. (A) GFP and mCherry expression were measured by FACS as described in the text at the indicated days after incubation with doxycycline as well as UT (untreated). (B) The indicated transcripts were quantified by RT-PCR after doxycline treatment to induce Cre synthesis. (C) Corresponding protein expression of the transcripts measured in (B) were determined by western blotting and quantified. The signals were quantified and graphically displayed as a percent of their value in untreated cells ($n = 3$). Data presented represent the mean ± SD.

Doxycycline (48 h)	
%GFP + mCherry+	**Number of Clones**
90+	5
49–89	7
0–30	76
Best Candidates	
Clone ID	**%GFP + mCherry+**
b.E8	99.4
b.A10	99.2
b.H8	96.5
b.H4	90.8
a.D6.1	90.8
a.D4	83.3
a.D6.2	83.3
b.E2	78.4
a.D6.3	78.4
a.A7	77.2
a.F5	64.4
a.A9	46.8

TABLE 1: Isolation and characterization of single cell clones.

expressed about twice as much *Grp170* mRNA compared with the nontransformed MEFs (Supplemental Figure S2D). In keeping with increased transcript levels, the bulk culture of transformed MEFs possessed three to four copies of the *Hyou1* locus compared with the nontransformed cells, which had two copies of this gene (see above). It was noteworthy, however, that Grp170 protein levels remained near that of the nontransformed cells, although transcript levels were much higher. These results might be consistent with an autoregulatory feedback system, which has been reported for BiP and cytosolic Hsp90 (Gülow *et al.*, 2002; Cheng *et al.*, 2010). As shown in Supplemental Figure S2D, the A10 clone expressed *Grp170* transcript levels that were similar to that of the nontransformed MEFs, whereas the E8 cells had about half the amount of *Grp170* transcript, indicating that this reduction in protein level did not adversely affect MEF viability.

Doxycycline treatment of the A10 and E8 clones resulted in a significant reduction in *Grp170* transcripts, which was apparent at day 3 of doxycycline treatment (Figure 2A). Protein levels began decreasing within 1 d and dropped precipitously to less than 5% by day 4 and 6 in the A10 and E8 clones, respectively (Figure 2B). Unlike the bulk cultures (see above), there was no "rebound" expression of Grp170 protein over 7 d. Moreover, as Grp170 protein levels diminished, cells began lifting off the dishes and were unable to exclude Trypan Blue (unpublished data). In accordance with these data, viability of both cell lines began to decrease within 1 d of doxycycline treatment and continued to fall as Grp170 protein levels decreased (Figure 2, B–C). Cell cycle analyses revealed that cell death was not accompanied by arrest at any particular phase of the cell cycle (unpublished data). Together, in keeping with our inability to isolate stable clones that were deficient in Grp170 expression (see above), the cells in both the A10 and E8 clones died as Grp170 was progressively depleted, despite the concurrent, robust up-regulation of Sil1, the other ER exchange factor for BiP (Figure 2D).

Loss of Grp170 results in dysregulated BiP function

We next examined a number of ER functions to understand why cells die as Grp170 is depleted. We first focused on BiP, given that Grp170 is a NEF for BiP, Grp170 shares a number of clients with BiP, and all of BiP's functions – other than its contribution to ER calcium stores (Lievremont *et al.*, 1997) – are adenosine nucleotide-dependent (Behnke *et al.*, 2014).

Under homeostatic conditions, a pool of BiP is AMPylated (Chambers *et al.*, 2012). This reversible modification provides an inactive reservoir of BiP that can be rapidly reactivated by ER stress (Perera and Ron, 2023) before the UPR can restore homeostasis by transcriptionally and translationally up-regulating a suite of resident ER chaperones and folding enzymes (Ron and Walter, 2007). In both the A10 and E8 clone, loss of Grp170 resulted in a rapid disappearance of AMPylated BiP (Figure 3, A and B). Activating this pool of BiP suggests an increased demand for BiP. Therefore, we next explored BiP's best understood function, the binding to a nonnative protein client. Because preliminary transient transfection experiments with BFP indicated that a significantly higher percent of the E8 clones were transfected than the A10 clone, we focused on the E8 clone to obtain quantitative data, but results were verified with the A10 clone where indicated.

The nonsecreted Ig light chain variant, NS1 κ light chain, is an established BiP client whose folding requires assembly with Ig heavy chains (Cowan *et al.*, 1974). Therefore, the interaction of BiP with unassembled NS1 κ light chains was determined by immunoprecipitation-coupled western blotting in cells treated with doxycycline for 5 d, which is sufficient to deplete ~90% of Grp170 protein compared with untreated cells (Figure 2B). As shown in Figure 4A, we detected greatly enhanced BiP association with NS1 under steady state conditions in the doxycycline-treated/Grp170-depleted cells. Because NS1 has a single ~100 amino acid domain that folds poorly (Skowronek *et al.*, 1998), this likely represents stabilization of binding as opposed to the binding of multiple BiP molecules. To determine whether loss of Grp170 stabilized BiP binding to other clients, we examined the turnover of the Null Hong Kong (NHK) variant of α1-anti-trypsin, because the retrotranslocation of this ERAD client to the cytosol for proteasomal degradation is dependent on BiP release (Inoue and Tsai, 2016). Consistent with defects in client release from BiP, pulse-chase experiments conducted on cells treated with doxycycline for 5 d revealed that NHK turnover was slowed (Figure 4B).

Unlike BiP, which binds short hydrophobic sequences in unfolded proteins, GRP170 preferentially associates with longer amino acid sequences in its clients that are rich in aromatic residues and have a propensity to form protein aggregates (Behnke *et al.*, 2016). Notably, the introduction of a GRP170 binding site into the unfolded domain of an Ig heavy chain resulted in the formation of insoluble aggregates in human HEK293T cells (Behnke and Hendershot, 2014; Behnke *et al.*, 2016), even though BiP is able to bind this domain (Hendershot *et al.*, 1987). Therefore, to determine whether BiP might be trapped in insoluble aggregates when Grp170 was deleted in the MEFs, we induced Cre expression and resolved proteins in the lysates into detergent-soluble and -insoluble fractions 3–6 d after doxycycline treatment. As Grp170 levels fell, BiP began to accumulate in the detergent-insoluble fraction (Figure 5). In both mammalian and yeast cells, the Z-variant of α1antitrypisin (A1PiZ) is a BiP substrate that forms insoluble, ordered polymers in the ER (Brodsky *et al.*, 1999; Schmidt and Perlmutter, 2005) and also interacts with Grp170 in mammalian cells (Schmidt and Perlmutter, 2005). To test the effects of Grp170 loss on this substrate, a plasmid encoding A1PiZ was introduced into untreated or doxycycline-treated E8 cells, and the protein was analyzed on day 5 after the

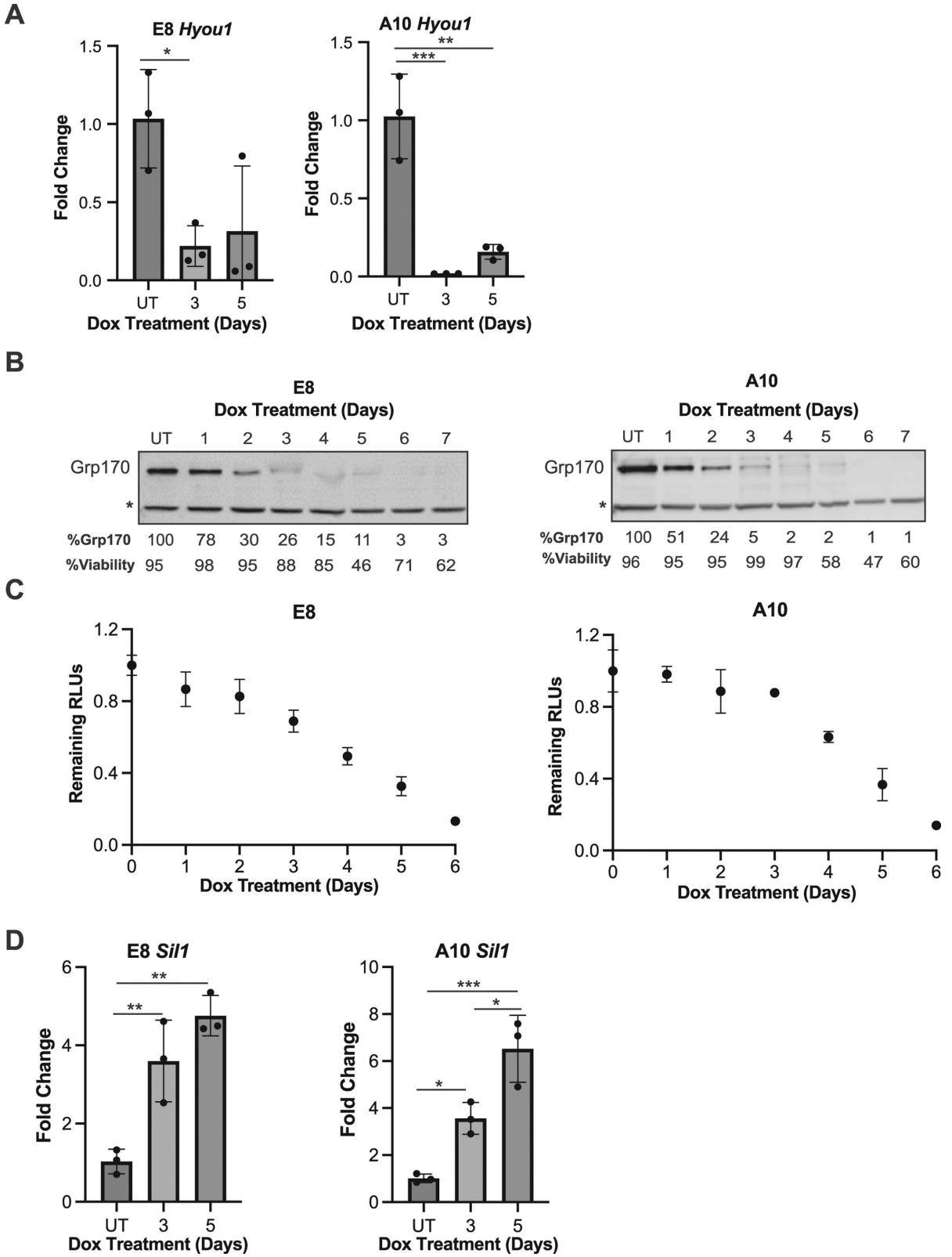

FIGURE 2: Inducible expression of Cre recombinase in single cell clones of *Hyou1*$^{fl/fl}$ MEFs leads to loss of Grp170, which decreases cell viability. (A) The expression of *Hyou1* transcripts were measured in the E8 and A10 clones after Cre induction ($n = 3$). (B) The resulting effect on Grp170 protein expression was assessed by western blot with levels relative to untreated (UT) cells displayed below each time point. A nonspecific band is indicated (*). (C) Cell viability was determined each day after Cre induction using a Cell Titer-Glo assay. Signals are expressed relative to that in untreated cells (UT) ($n = 3$). (D) Transcripts for *Sil1*, the other ER NEF, were quantified by RT-PCR after loss of *Grp170* in each clone. Data represent the mean ± SD; *$p < 0.05$, **$p < 0.01$, ***$p < 0.001$.

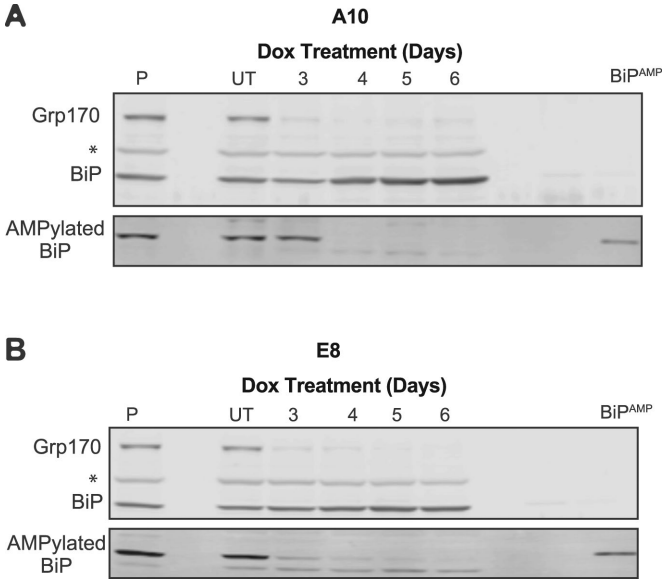

FIGURE 3: As Grp170 levels fall, AMPylated pools of BiP are reactivated to increase the pool of functional BiP. Cells from the (A) A10 and (B) E8 clone were incubated with doxycycline for the indicated days, and cell lysates were prepared for western blotting. The top panel portrays a membrane blotted with a combination of anti-Grp170 and anti-BiP, whereas the bottom panel is from a membrane blotted with a monoclonal antibody specific for AMPylated BiP. An aliquot of recombinant AMPylated BiP was loaded on the right of the gel, and the parental clone (P) was loaded to the left ($n = 3$). A band migrating between Grp170 and BiP (*) was detected with the anti-Grp170 rabbit polyclonal serum, although its identity is unknown.

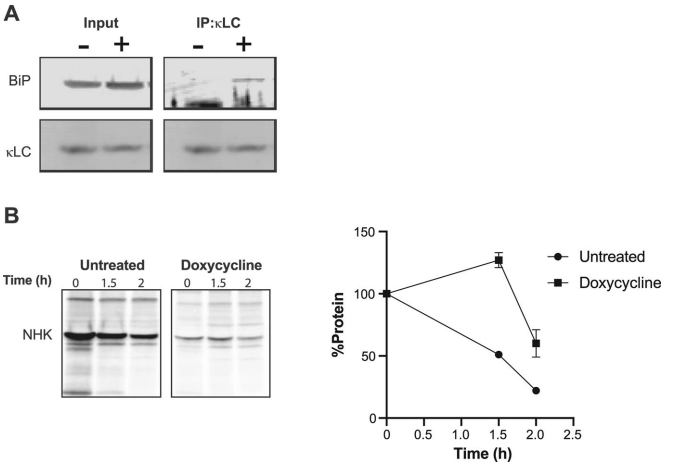

FIGURE 4: Loss of Grp170 increases steady-state BiP binding to an unfolded client and slows its degradation. (A) Cells from the E8 clones were transfected with an expression vector encoding the NS1 LC 4 d after incubation with doxycycline (+), and lysates were prepared the following day. Untreated cells (–) served as a control. The mouse κ LC was immunoprecipitated from lysates, resolved on reducing SDS-gels, transferred, and blotted with anti-BiP or anti-κ, $n = 3$. (B) E8 cells that had been treated with doxycycline or left untreated were transfected with an expression vector encoding the NHK variant of α1AT. The next day, the cells were pulsed with [^{35}S]-labeled methionine and cysteine for 30 min before chasing for the indicated times. Lysates were prepared, and 90% of the lysate from a p60 dish was immunoprecipitated with anti-α1AT antibody for each time-point and electrophoresed on reducing SDS-polyacrylamide gels. Signals were determined on a phosphorimager and represented as a percentage of that observed at the start of the chase ($t = 0$). Data represent the mean ± SD ($n = 2$).

initial addition of doxycycline. As shown in Figure 5B, A1PiZ was primarily insoluble in both treated and untreated cells. However, in the absence of Grp170, significantly more A1PiZ was found in the pellet fraction suggesting that Grp170 is required to either limit aggregation formation or to promote A1PiZ aggregate turnover. Additionally, A1PiZ total protein levels were significantly higher when cells were treated with doxycycline, which is consistent with Grp170 playing a role in A1PiZ quality control, either directly or in a BiP-mediated manner.

An unresolved ER stress response in Grp170-depleted MEFs culminates in apoptotic cell death

When BiP levels become insufficient to perform its various functions in maintaining ER homeostasis, the chaperone is recruited from ER-localized UPR transducers, Ire1, ATF6, and PERK, to aid in protein refolding/maturation or to target nonnative proteins for ERAD (Bertolotti *et al.*, 2000; Shen *et al.*, 2002). This allows activation of the UPR transducers and signals a complex transcriptional and translational response to restore homeostasis, in part by up-regulating BiP (Walter and Ron, 2011; Hetz *et al.*, 2020). To further determine whether Grp170 loss adversely impacted BiP availability, the A10 and E8 clones were examined for evidence of UPR activation (Figure 6, A and B; Supplemental Figures S3 and 4). As described below, targets of each of the three arms of this ER stress response were up-regulated at both the transcriptional (Figure 6A; Supplemental Figure S3) and translational (Figure 6B; Supplemental Figure S4) levels as Grp170 was depleted. Although there is significant crosstalk between the three downstream targets of the various transducers (Ron and Walter, 2007; Walter and Ron, 2011), several transducer-specific responses were observed. First, activation of Ire1 triggered splicing of the transcript encoding the *Xbp1* transcription factor (s*Xbp1*), thereby increasing Hrd1 levels (Yamamoto *et al.*, 2008). Second, ATF6 activation resulted in BiP up-regulation (Yoshida *et al.*, 1998; Wang *et al.*, 2000). Third, activation of PERK leads to the phosphorylation (p-eIF2α) and inhibition of eIF2α translational activity, which paradoxically increases ATF4 and CHOP synthesis. Notably, the levels of all these targets continued to increase through day 5 of doxycycline treatment, but by day 7 some of them decreased, with PERK transcriptional targets returning to basal levels (Figure 6A). Unexpectedly, p-eIF2α protein levels remained high (Figure 6B). Through a feedback loop, the translational inhibition caused by eIF2α phosphorylation drives synthesis of the Gadd34 phosphatase, which acts on p-eIF2α to restore translation (Harding *et al.*, 2009). In keeping with prolonged eIF2α phosphorylation, lower levels of Gadd34 protein were also evident at day 5 and 7 of doxycycline treatment (Figure 6C; Supplemental Figure S4). Therefore, in spite of prolonged phosphorylation of eIF2α, the PERK pathway was no longer able to drive transcription of its targets ATF4 or CHOP at later time points. Importantly, stable expression of wild-type GRP170 in dox-treated E8 MEFs reduced BiP expression to near control levels (Supplemental Figure S4C), confirming that loss of Grp170 is responsible for the observed UPR activation.

In addition to a well-established role for CHOP in ER stress-associated cell death (Zinszner *et al.*, 1998), a number of caspases are also activated by unresolved UPR activation (Iurlaro and Muñoz-Pinedo, 2016). One route by which apoptotic cell death

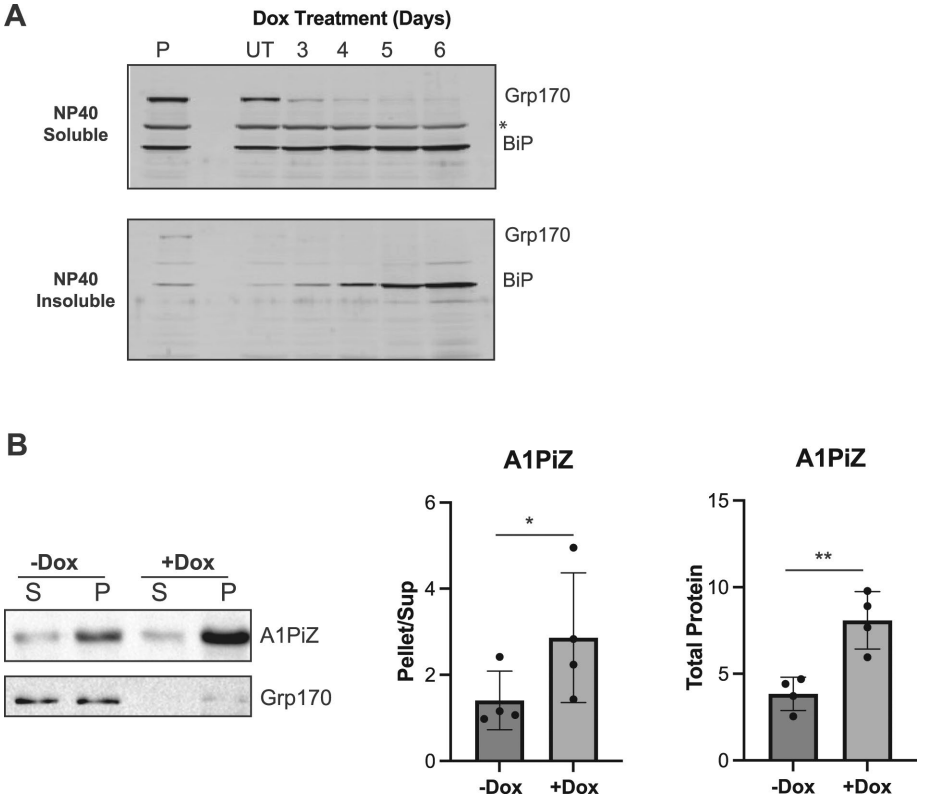

FIGURE 5: The relative percent of an aggregation-prone protein and BiP in the insoluble fraction increases as Grp170 is depleted. (A) Cre recombinase expression was induced in E8 cells for the indicated days. Cells were lysed with NP40 buffer and centrifuged at 20,000 g to separate NP40 soluble and insoluble material. The insoluble material was extracted by heating in Laemmli buffer and sonication. The samples loaded on the NP-40 insoluble gel (bottom) are six times that loaded on the NP40 soluble gel (top). After electrophoresis and transfer, membranes were blotted for BiP and Grp170 ($n = 3$). A nonspecific band is indicated (*) (B) Cre recombinase expression was induced in E8 cells which were transfected with an expression plasmid for A1PiZ. Cells were harvested at 5 d postdox induction (48 h posttransfection). Cells were lysed and lysate was centrifuged at 100,000 g for 1 h to separate soluble and insoluble material. Samples loaded on the gel correspond to 20% of the supernatant and the entire pellet fraction. After electrophoresis and transfer, membranes were probed with antibodies against A1PiZ and Grp170. Data represent the mean ± SD; *$p < 0.05$, **$p < 0.01$ ($n = 4$).

occurs is via activation of caspase-3, downstream of Ire1 activation (Fribley *et al.*, 2009). Indeed, consistent with the progressive onset of cell death as Grp170 was depleted (Figure 2, B and C), caspase-3 cleavage was detected as early as d 5 postdoxycycline treatment and became significantly more prominent by d 7 (Figure 6D).

Loss of Grp170 alters ER morphology

Sustained ER stress can disrupt ER morphology (Ng *et al.*, 2000; Gardner *et al.*, 2013). To examine the effects of Grp170 loss on ER structure in MEFs, we stained fixed doxycycline-treated and control cells with an anti-KDEL antibody, which recognizes the ER retention sequence found on the C-terminus of many soluble resident ER proteins (Munro and Pelham, 1987), and can be used to visualize the ER. As presented in Figure 7A, ER structure at day 5 and 7 postdoxycycline treatment appeared more collapsed than the untreated or day 3 cells. Notably, the cells at later time-points were also smaller, which was verified by quantifying the cytosolic GFP signal (Figure 7B). We next measured the levels of Climp63, a cytoskeleton-linking membrane protein (Klopfenstein *et al.*, 2001) that helps maintain ER morphology and is required for ER sheet formation (Shibata *et al.*, 2010; Gao *et al.*, 2019). As Grp170 levels fell, Climp63 expression was unchanged at day 3 but was significantly reduced at day 5 and 7 (Figure 7C), consistent with ER collapse. Decreased Climp63 expression may be due to reduced protein synthesis (see, for example, the NHK signal in Figure 4B), which we attribute to sustained eIF2α phosphorylation and reduced Gadd34 levels (Figure 6).

DISCUSSION

In this study, we describe the isolation and characterization of a cell-based, inducible knockout system to investigate the functional significance of Grp170, an ER resident molecular chaperone that exhibits both holdase and NEF activities. The importance of this chaperone was previously indicated by failed attempts to construct homozygous null mice (Kitao *et al.*, 2001) and by the catastrophic effects on kidney function observed when Grp170 was depleted from nephrons in adult mice (Porter *et al.*, 2022). However, its requirement at the cellular level had not been established nor were its effects on various ER functions. Using MEFs with regulated ablation of Grp170, we discovered that – other than BiP (Luo *et al.*, 2006; Paton *et al.*, 2006) – Grp170 is the only ER chaperone that is essential for cell survival. Although Grp94 is required for mouse development, its depletion is tolerated in a number of tissues and cell lines (Wanderling *et al.*, 2007). At the molecular level, murine Grp170 depletion disrupts several critical BiP functions, including increased steady-state BiP substrate binding, consistent with defects in Grp170-dependent substrate release, and a defect in ERQC, resulting in the accumulation of misfolded proteins as well as an increase in the insoluble fraction of BiP and an aggregation-prone protein in the ER. In keeping with the hypothesis that the loss of Grp170 impinges on BiP availability, BiP deAMPylation, which provides a rapid restoration of functional BiP (Perera and Ron, 2023), was evident when ~25% of Grp170 remained. Thus, its plausible that the cells die at later times, as Grp170 is further depleted, due to insufficient levels of BiP that are required to execute its essential functions.

Cell death may also or alternatively arise due to unresolved UPR activation (Iurlaro and Muñoz-Pinedo, 2016). Because the UPR transducers are regulated by BiP binding (Bertolotti *et al.*, 2000; Shen *et al.*, 2002), diminished BiP repression of the transducers might affect cell death. However, we observed unexpected irregularities in this stress response as Grp170 levels fell, which might further diminish the ability of the UPR to restore homeostasis. For example, eIF2α phosphorylation was sustained, and the resumption of translation was impaired as judged by decreased synthesis of NHK in the pulse-chase experiment, loss

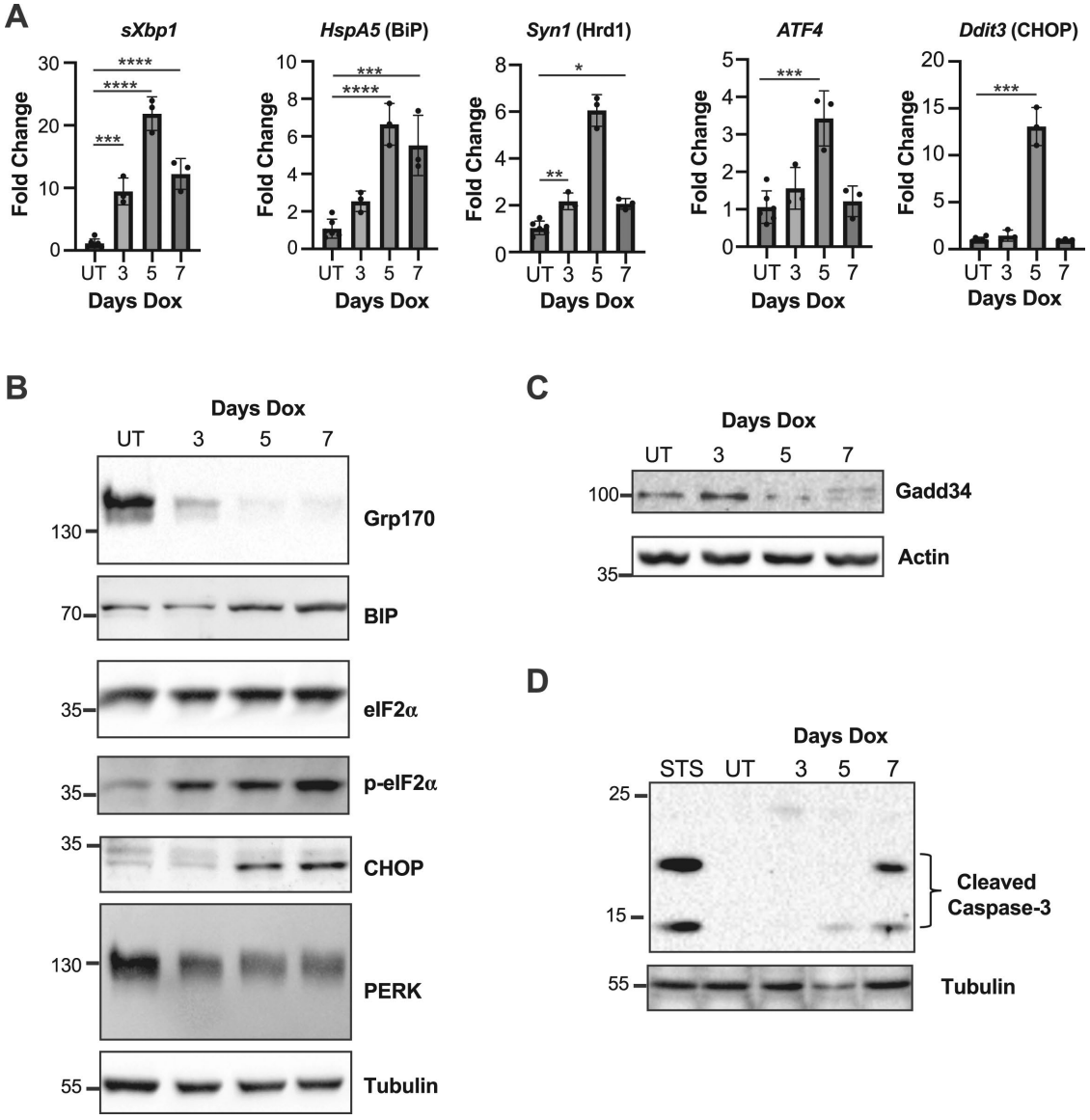

FIGURE 6: The UPR is activated in the absence of Grp170. (A) The expression of UPR target transcripts was measured in the E8 clone after Cre induction for the indicated days by qPCR ($n = 3$). Data represent the mean ± SD; *$p < 0.05$, **$p < 0.01$, ***$p < 0.001$, ****$p < 0.0001$. (B) Western blot analysis was also performed for UPR targets (B), Gadd34 (C), an apoptotic marker (D), and loading controls (actin or tubulin). For (D) cells were also treated with 1 μm staurosporine (STS) as a positive control for apoptosis. Representative images are shown.

of Gadd34 protein, which is the phosphatase responsible for dephosphorylation of eIF2α, and reduced expression of Climp63, a structural component of the ER. Another possibility for the lethality associated with Grp170 depletion is that an essential Grp170-dependent protein client(s) fails to mature properly in its absence. Currently, only a handful of proteins that transit the secretory pathway have been identified that directly interact with Grp170 (Lin *et al.*, 1993; Behnke and Hendershot, 2014), and at least some of them are likely aggregation-prone in the absence of Grp170 (Behnke *et al.*, 2016). Overall, it is reasonable to assume that any or all these effects contribute to the cellular requirement for Grp170.

In contrast to the apparent essential nature of Grp170 in mammalian cells, the yeast homologue of GRP170, Lhs1, can be deleted and the cells continue to divide normally. However, similar to our observations in mammalian cells, loss of Lhs1 induces the UPR. Δ*lhs1* yeast also exhibit a subtle, temperature sensitive defect in ER protein translocation (Craven *et al.*, 1996), and – consistent with the current study – a defect in the turnover of a misfolded protein in the ER (Buck *et al.*, 2013). Both higher eucaryotic cells and yeast possess a second ER localized NEF, Sil1, which is a functional analogue but lacks structural similarities with Grp170/Lhs1 and does not bind unfolded clients (Behnke *et al.*, 2015). In yeast, loss of Sil1 induces a milder UPR relative to loss of Lhs1 and no obvious protein processing defect, whereas deletion of both Lhs1 and Sil1 in combination is synthetic lethal (Tyson and Stirling, 2000). Interestingly, the Δ*lhs1*Δ*ire1* double deletion is synthetically lethal in yeast but is rescued by Sil1 overexpression (de Keyzer *et al.*, 2009),

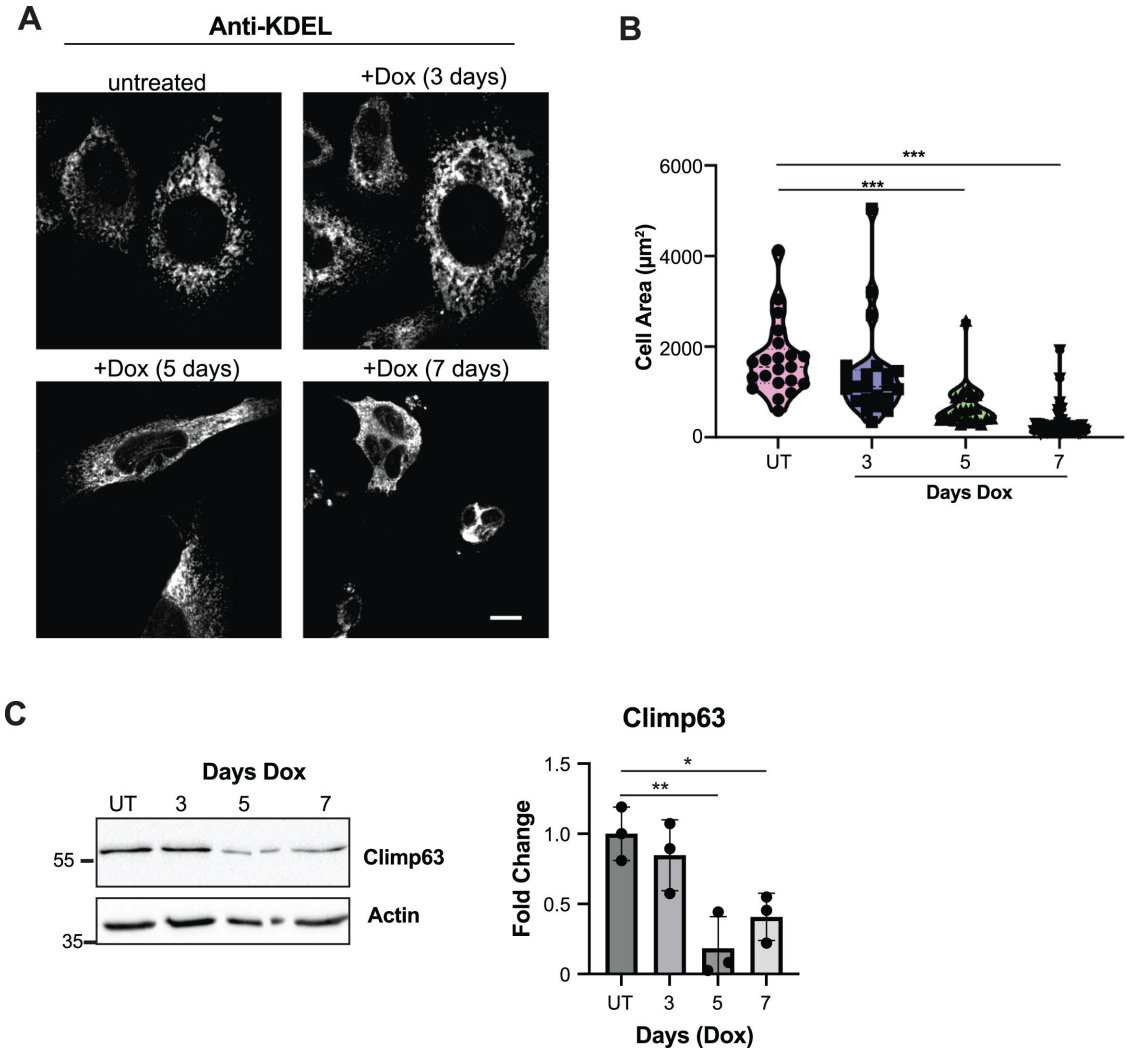

FIGURE 7: ER morphology is altered as Grp170 is depleted. (A) E8 cells grown on coverslips were treated for the indicated times to induce Cre-lox editing of Grp170. Cells were stained for KDEL followed by anti-Rabbit 647 secondary antibody to mark the ER. Scale bar in the bottom right panel is 10 µm (Bottom). (B) Whole cell area was quantified using Nikon NIS-Elements software. Violin plots depicting the individual data points as well as the median, and first and third quartiles are plotted, ***$p < 0.0001$ ($n = 21–37$). (C) Protein lysates from the E8 clone treated with doxycycline for the indicated days were subject to western blot and probed with anti-Climp63 antibody. Data represent the mean ± SD; *$p < 0.05$, **$p < 0.01$ ($n = 3$).

suggesting that NEF activity is the essential function in yeast. It is, therefore, also interesting to note that the essential function of the cytosolic Hsp70 NEF, Sse1, in yeast, is thought to be its protein disaggregase activity when operating in conjunction with an Hsp70 (Garcia *et al.*, 2017). Nevertheless, although we show that Sil1 levels increase when murine Grp170 is depleted (Figure 2D), these NEFs/chaperones either exhibit independent essential functions in higher cells, or the level of Sil1 induction we observed was insufficient to rescue the loss-of-function phenotypes upon Grp170 ablation.

As opposed to the inability to produce a Grp170 null mouse (Kitao *et al.*, 2001), the loss of Sil1 results in the production of viable progeny, although these mice phenocopy many of the symptoms associated with disease-associated mutations in SIL1 that result in Marinesco-Sjögren syndrome (Zhao *et al.*, 2005; Ichhaporia *et al.*, 2018). Sil1 knockout in mice is also accompanied by UPR activation, leading to increased levels of Grp170 and again revealing nonredundant aspects of these two ER NEFs. To avoid the catastrophic effects of complete Grp170 loss during development, we recently generated an inducible, kidney-specific Grp170 knockout mouse. Loss of Grp170 in the mouse kidney resulted in defects in salt and water homeostasis, which resulted from widespread kidney injury (Porter *et al.*, 2022). As observed in the current study, there was strong induction of the UPR, alterations in ER morphology, and ultimately an apoptotic response. Although the cell-based inducible knockout system reported here provides a more experimentally tractable system to understand how loss of Grp170 affects cell physiology, future work will better define how other components of the proteostasis network are affected upon the loss of Grp170. These data can then be compared with parallel ongoing efforts using our in vivo model to study Grp170 biology in other organ systems.

Another advantage of the new cell-based inducible Grp170 knockout system is that the phenotypic consequences of

uncharacterized amino acid variants and polymorphisms in the gene encoding GPR170 on cellular physiology can now be studied. Consistent with a role of Grp170 in supporting the biogenesis of IgM antibodies (Lin *et al.*, 1993), mutations in the *HYOU1* locus were identified in patients presenting with combined immunodeficiency as well as hypoglycermia (Haapaniemi *et al.*, 2017). This latter symptom might be associated with the importance of GRP170 function during insulin maturation in the ER. Moreover, Grp170 limits aggregation of the Akita mutant form of insulin in mice by targeting this misfolded substrate for degradation via ER-phagy (Cunningham *et al.*, 2017, 2019). It is thus intriguing that polymorphisms in *HYOU1* are associated with diabetes in Pima Indians (Kovacs *et al.*, 2002). GRP170, also known as ORP150, can be regulated independent of the UPR by proteasomal inhibition during hypoxic conditions (Zong *et al.*, 2016). Recent studies have additionally implicated GRP170 in tumorigenesis associated with several cancers, including bladder, papillary thyroid, and breast. Of note, overexpression of GRP170 in these cancers correlates with poor outcomes and increased cell mobility and proliferation (Hao *et al.*, 2021; Lee *et al.*, 2021; Wang *et al.*, 2021, 2023). Furthermore, a requirement for GRP170 NEF activity in both cholera toxin and polyomavirus pathogenesis was uncovered, because GRP170 releases BiP from the toxin/virus, which is needed for its retrotranslocation from the ER to the cytosol where it produces its pathogenic effects (Inoue and Tsai, 2015; Williams *et al.*, 2015). Finally, by using several models, our group determined that Grp170 regulates the quality control and early biogenesis of the ENaC (Buck *et al.*, 2013), a major regulator of ion homeostasis and blood pressure.

Overall, the findings reported here shed light on the essential cellular functions played by Grp170, including a major impact on BiP's nucleotide-dependent chaperone activities, and provide a foundation for future studies to determine Grp170 substrate specificity, identify structure-function relationships in this dual-purpose chaperone, and define the defects associated with disease-causing alleles in the *HYOU1* locus.

MATERIALS AND METHODS

Request a protocol through *Bio-protocol*.

Mice

LoxP sites were engineered in introns 1 and 24 of the *Grp170* (*Hyou1*) gene of C57Bl/6 mice to generate *Hyou*$^{LoxP/LoxP}$ mice, which were previously described (Porter *et al.*, 2022). Both male and female *Hyou*$^{LoxP/LoxP}$ mice were fertile, as were their offspring. The mice were housed and treated in accordance with the Animal Use and Care Committee and the Animal Research Center at St. Jude Children's Research Hospital, adhering to the National Institutes of Health guidelines. At weaning, DNA was isolated from mouse tail snips using DNeasy Blood & Tissue Kit (Qiagen, Valencia, CA) and genotyped. Primers for the wild-type allele and for the disrupted allele are listed below.

Oligos used for genotyping mice and MEF cells:

For detection of	Forward primer	Reverse primer
Lox-P rearrangement	GAGGATGGAGCAGCCGTC	CCCCGAGACAGGGTTTCTCT
Intact intron 1	GAGGATGGAGCAGCCGTC	GACCCTCGAAATCGGCTCAA
Intact intron 24	CGGTGAATGTGGTGGCCTTT	CCCCGAGACAGGGTTTCTCT

Isolation of MEFs from Hyou$^{LoxP/LoxP}$ mice and transformation

Timed pregnancies were conducted using male and female *Hyou*$^{LoxP/LoxP}$ mice (Porter *et al.*, 2022). Embryos were surgically obtained at e12.5 d for the isolation of MEFs using standard procedures (Kamijo *et al.*, 1997). Briefly, organs from e12.5 embryos were removed and transferred to conical tubes containing DMEM/HEPES media (DMEM 4.5g/L glucose supplemented with 2 mM L-Glutamine, Penicillin/Streptomycin, 0.1 mM nonessential amino acids, 5.5 μM 2-mercaptoethanol, and 10% fetal bovine serum [FBS]). Organs were dispersed into single cells and plated on p100 dishes.

After three passages to select for fibroblasts, aliquots of *Grp170*$^{LoxP/LoxP}$ non-transformed MEFs were stored in liquid nitrogen, which are referred to as primary MEFs in this manuscript. To obtain transformed MEFs, the primary MEFs were plated, and at 80% confluency they were transfected with 4 μg of SV40 DNA per p60 dish using the Genecellin transfection reagent per manufacturer's recommendations. Media was changed 24 h later. Cells were passaged to allow SV40-immortalized cells to outgrow nontransformed cells according to the Harding/Ron protocol (Harding *et al.*, 2000). These *Grp170*$^{LoxP/LoxP}$/SV40-transformed MEFs are referred to as parental MEFs.

Cell Culture

MEF cells were maintained at 37°C and 8% CO_2 in Dulbecco's Modified Eagle's Medium (DMEM) (Corning, 15013-CV) supplemented with 10% (vol/vol) FBS – TET Tested (Biotechne S10350), 55 μM nonessential amino acids (Life Technologies 11140050), 1 × 2-mercaptoethanol (Life Technologies 21985023), and 1% l-glutamine (Corning, 25-005-CI). To passage cells, TrypLE (Life Technologies) was used. HEK293T cells used for transient expression of the inducible Cre vector were maintained at 37°C and 5% CO_2 in DMEM (Corning, 15013-CV) supplemented with 10% (vol/vol) FBS (Atlanta Biologicals S11550) and 1% l-glutamine (Corning, 25-005-CI). For all lines, cells were periodically tested for mycoplasma to ensure only mycoplasma-free cells were used.

Creation of an inducible Cre construct and introduction into Grp170$^{LoxP/LoxP}$ MEFs

The pSJL224 lentivirus backbone vector was obtained from the SJ vector core. This vector encodes a constitutive eGFP followed in-frame by the Tet-On 3G gene separated by a P2A ribosome cleavage site. The mCherry gene was introduced down-stream of the TRE 3G promoter, which was followed by a 2A peptide sequence and the Cre recombinase gene. This construct was designed to provide expression of both mCherry and Cre only in the presence of doxycycline (Supplemental Figure S1A). An initial test of this construct was performed by introducing it into two dishes of HEK293T cells using the Genecellin transfection reagent. Twenty-four hours later, one dish was treated with 3 μg/ml doxycycline in sterile water. The following day, GFP and mCherry expression were detected using FACS analysis (BD Biosciences Fortessa).

Lentiviruses were produced by combining standard third generation packaging and envelope plasmids with Cre-modified pSJL224 backbone vector in 0.25M calcium in sterile water. The transfection mixture was incubated at room temperature for 10–15 min and then added dropwise to HEK293T cells on a p100 dish. Cells were incubated at 37°C in 5% CO_2 for 16–20 h. Media was then aspirated, and 5 ml of fresh DMEM was added. Twenty-four hours later, culture supernatants containing virus were harvested and passed through a 0.45 μM polyvinylidene fluoride (PVDF) filter (Millipore, SLHV033RS). Viral titers were calculated and an MOI of one was used for transduction. The virus-containing media was mixed with DMEM/polybrene (final concentration 6 μg/ml) up to 5 ml and was added to *Grp170*$^{LoxP/LoxP}$ MEFs on a p100 dish. Twenty-four hours later, an additional 5 ml of DMEM was added to dilute lentiviral toxicity. After 1 wk, a bulk culture of GFP$^+$, mCherry$^-$ cells was isolated by cell sorting (BD Biosciences Aria).

Isolation of single cell clones with tight regulation of Cre

The bulk culture of GFP$^+$ Hyou$^{LoxP/LoxP}$ MEFs were resorted to obtain the brightest 15% GFP$^+$ cells that were mCherry$^-$ cells, and single cells were dispersed into 96-well plates. After expanding, 88 single-cell clones were identified. An aliquot of each was treated with 3 μg/ml doxycycline for 2 d, and the percent mCherry$^+$ cells in each clone was determined by FACS analysis (Table 1). Cells were genotyped using the primers listed above.

Stable expression of wild-type GRP170 in the Grp170 E8 MEF cell line

Wild-type human GRP170 was subcloned from pcDNA3.1 hGRP170 (Behnke and Hendershot, 2014) using the EcoR1 and HindIII restriction sites and ligated into the pcDNA4/TO plasmid, an integrating vector that contains a tetracycline (tet) inducible CMV promoter, using standard cloning procedures. Expression from pcDNA4/TO is repressed in the absence of doxycycline (tet) when the tet repressor (TetR) is present. However, the TetR is not expressed in the E8 MEFs, therefore the expression of hGRP170 is constitutive under these conditions. Next, E8 cells were transfected with pcDNA4/TO hGRP170 or pcDNA4/TO alone, as described above, with GeneCellin. Transfected cells were subject to selection for 3 wk in zeocin (500 μg/ml) containing media as described by the manufacturer (Thermo Fisher Scientific) to isolate stable integrants and then frozen for subsequent experiments. Expression of exogenous hGRP170 was confirmed in a pilot experiment by treating cells with doxycycline for 5 d to eliminate endogenous mouse GRP170, as described above. Cell lysates were subject to western blotting with anti-GRP170 antibody, and empty vector integrated/stable E8 cells served as a negative control.

In Supplemental Figure S4C, the E8 cells engineered to stably express hGRP170 or those with the integrated empty vector were treated with doxycycline for 7 d, which correlates with both elimination of endogenous Grp170 and maximal UPR activation. The cells were lysed, and western blots were performed for GRP170, BiP, or actin as a loading control as described above.

Fluorescence in situ hybridization

The Cytogenetic Shared Resource Laboratory at SJCRH designed a FISH assay to be used for this analysis. Purified *Hyou1* telomeric flanking fosmid DNA (WI1-2296B18) was used as a locus specific control. A 10 kb subclone corresponding to the genomic *Hyou1* sequence between the two LoxP sites was PCR-amplified from the *Hyou1* fosmid WI1-1167J13 clone using an initial primer pair followed by a nested primer pair listed below. This probe was used identify the cre-lox programmed deletion. After a 4-h colcemid incubation, the cells were harvested using routine cytogenetic methods. The slides were pretreated with Rnase A for 45 min before hybridization. After purification, the *Hyou1*-telomeric flanking fosmid DNA (WI1-2296B18) DNA was labeled with a red 580 dUTP (Enzo) by nick translation. The purified *Hyou1* 10 kb genomic subclone was labeled with a green 496 dUTP (Enzo). The *Hyou1* (red) fosmid and the *Hyou1* (green) 10 kb subclone probes were combined with sheared mouse cot DNA and hybridized to cells derived from the samples in a solution containing 50% formamide, 10% dextran sulfate, and 2X saline sodium citrate. After overnight hybridization, the cells were washed and stained with DAPI (1 μg/ml). Two hundred cells were analyzed for each of the experimental groups, and the numbers of intact versus deleted genes were determined. Cells in which the *Hyou1* gene is intact have paired red-green signals, while loci that have undergone the programmed deletion will have only the control flanking signals (red) present.

Primers used for isolating the genomic *Hyou1 probe*

	Forward primer	Reverse primer
First PCR	GAGGATGGAGCAGCCGTC	TCGTTGCTTGCTTGCTTTCT
Nested PCR	TTGAGCCGATTTCGAGGGTCC	AAGGCCACCACATTCACCGA

RNA expression studies

Total RNA was isolated from MEF cell pellets using RNeasy Plus Mini Kit (Qiagen), according to the company protocol. Two microgram total RNA was reverse transcribed using the High Capacity cDNA Reverse Transcription Kit (Applied Biosystems) and subjected to SYBR Green chemistry-based qPCR using the QuantStudio 3 Real-time PCR System (Applied Biosystems, Foster City, CA). Primers were obtained from Thermo Fisher Scientific. GAPDH was utilized as a reference gene control. Relative mRNA fold change was computed from the QuantStudio-generated Ct values by using the $2^{-\Delta\Delta Ct}$ method. Except in the case of Cre transcripts, mRNA values obtained from untreated cells were set to 100%, and values for the days after doxycycline addition were expressed relative to those of the controls. At least three biological replicates were performed, and each was assayed in triplicate. Statistical analyses were conducted using Prism 9 software package (GraphPad Software). When comparing more than two groups a one-way ANOVA was performed with Tukey's multiple comparisons test, where the mean of each group was compared with the mean of every other group.

Oligos for mRNA expression

Site	Forward primer	Reverse primer
GAPDH	*AAGGCTGTGGGCAAAGTCATCC*	*CTTCACCACCTTCTTGATGTCATC*
Sil1	*CTGCGCCACTTCCCCTAT*	*GCAAACATCTTCTCAGTGACCA*
Hyou1	*GAGGATCTTCGGGTATTTGGC*	*TGCCTTTGGACTCATAGTCGG*
HSPA5 (BiP)	*TGTGGTACCCACCAAGAAGTC*	*TTCAGCTGTCACTCGGAGAAT*
Cre Recombinase	*CGACCGGCAAACGGACAGAAG*	*GTCCAATTTACTGACCGTACACCA*
CHOP	*CCTAGCTTGGCTGACAGAGG*	*CTGCTCCTTCTCCTTCATG*
HspA5	*GGATCATCAATGAGCCTACAGC*	*ACCCAGGTCAAACACAAGGAT*
sXbp1	*GGTCTGCTGAGTCCGCAGCAGG*	*GAAAGGGAGGCTGGTAAGGAAC*
ATF4	*GCAAGGAGGATGCCTTTTC*	*GTTTCCAGGTCATCCATTCG*
*Actin*β	*GGCTGTATTCCCCTCCATCG*	*CCAGTTGGTAACAATGCCATG*
Hrd1	*AGCTACTTCAGTGAACCCC*	*TCTACAATGCCCACTGAC*

Transfections, western blotting, and immune reagents

E8 cells were plated with or without doxycycline for 3 d and then replated with the same conditions for 24 h before transfecting with the GeneCellin transfection reagent (BioCellChallenge, GC5000) according to the manufacturer's instructions. Cell pellets were disrupted using NP-40 lysis buffer (0.5 M Tris-HCl pH 7.5, 0.15 M NaCl, 0.5% DOC, 0.5% NP40 substitute, 0.002% sodium azide) supplemented with 0.1 mM phenylmethylsulfonyl fluoride and 1x Roche complete protease inhibitor tablets and clarified by centrifugation for 15 min at maximum speed in a refrigerated microfuge to produce clarified cell lysates. Equivalent amounts of total protein, as determined by Coomassie Protein Assay Reagent (Thermo Scientific, 23200) were loaded on gels. In the experiments to separate NP40 soluble and insoluble proteins, the clarified lysate corresponded to the soluble material and the resulting pellet was solubilized by heating in sodium dodecyl sulfate (SDS) sample buffer at 95°C for 5 min followed by water bath sonication. The amount of insoluble pellet loaded was six times that of the corresponding soluble sample. For A1PiZ solubility assays, E8 cells were treated with doxycycline, transfected and harvested on day 5 postdox treatment (48 h posttransfection). Cells were lysed in 1% Tx-100 buffer (10 mM Tris-Cl pH 8.0, 140 mM NaCl, 1 mM EDTA, and 1% Tx-100) plus proteasome inhibitors. Lysate was centrifuged to clear at 1000 g for 5 min, supernatant was transferred to a new tube and protein was normalized using a BCA assay. Normalized lysate was centrifuged at 100,000 g for 1 h at 4°C. Supernatant was collected and the pellet was resuspended in 15 µl SDS sample buffer. In all cases, samples were electrophoresed under reducing conditions on SDS-polyacrylamide gels and transferred to PVDF membranes (Millipore #IPFL00010). Membranes were blocked with either 4% nonfat milk or fish gelatin (Sigma #G7041-100G) for 30 min at room temperature and incubated overnight in primary antibodies on an orbital rocker at 4°C. Membranes were serially washed in Tris buffered saline followed by Tris buffered saline with 0.1% Tween20 and incubated in secondary reagents for 1 h at room temperature on an orbital rocker. Finally, membranes were serially washed again and imaged on a Li-Cor CLx imager and visualized using Image Studio (LI-COR Biosciences, Lincoln, NE) and fluorescent secondary antibodies. Alternatively, when HRP-conjugated secondary reagents were used, the membranes were incubated in ECL Western Blotting Substrate (Pierce #32106) and developed on film (Denville Scientific #E3018) or imaged on a BioRAD Universal Hood II Imager and quantified using ImageJ 1.51 h software (National Institutes of Health). Rabbit antirodent BiP (Hendershot *et al.*, 1995) and GRP170 (Behnke *et al.*, 2014) were previously produced in our lab. Immune serum specific for Cre (Cell Signaling, 12830S), CHOP (Cell Signaling #2895S) Hsc70 (Santa Cruz, SC-7298), eIF2α (#5324S) and p-eIF2α (Cell Signaling 9721L), PERK (Cell Signaling #3192), tubulin (Proteintech 66031), Cleaved-Caspase 3 (cell signaling #9661S), OS-9 (Abcam ab109510), A1PiZ (Agilent, A0012), and Climp63 (Bethyl Laboratories, A302-257A) were purchased from commercial venders. A monoclonal antibody specific for AMPylation and AMPylated recombinant BiP were kind gifts of the Itzen laboratory (Hamburg University). Secondary immune reagents were used at a dilution of 1:10,000 (antimouse; Cell Signaling #7076S) or antirabbit (#7074S). Values for protein signals were normalized to either Revert Total Protein Stain (Li-Cor, 926-11021), actin or tubulin and expressed relative to the untreated samples, which were set to 100%. For Cre protein, the d 2 value was set to 100%, and subsequent days of treatment were expressed relative to the d 2 value. At least three biological replicates were performed.

Pulse-chase experiments

To measure the effects of Grp170 loss on an ERAD client, E8 cells were transfected with a vector encoding the NHK variant of α1AT that were either left untreated or incubated with doxycycline 4 d as described for NS1 experiments above. Cells were preincubated in 2 mL labeling media consisting of 1x DMEM without Cys and Met (Cys-/Met-; Corning, 17-204CI) supplemented with 10% Tet free FBS dialyzed against phosphate-buffered saline (PBS), 1% L-glutamine, and 1% antibiotic/antimycotic at 37°C for 30 min and then labeled with Express [^{35}S] Labeling Mix (PerkinElmer, NEG072-007) for 15 min. After labeling, cells were put on ice, rinsed with PBS and 2 ml of complete growth media supplemented with cold methionine and cysteine was added to the chase dishes, which were returned to 37°C and 8% CO_2 for the indicated times. At the end of the chase period, cells were washed on ice 2x with PBS and then lysed with the NP40 buffer and clarified as described for western blotting. Samples were incubated with rabbit anti-α1-antitrypsin (A0409-1VL, Millipore Sigma) overnight at 4°C followed by Protein A agarose beads (CA-PRI-0100, Repligen) for 1 h the following morning. Isolated protein was eluted with reducing Laemmli buffer by heating at 95°C for 5 min. Proteins were separated by SDS–PAGE and transferred to PVDF membrane as described for western blotting. Dried membranes were exposed to BAS storage phosphor screens (Cytiva, 28956475) and scanned using a phosphorimager

(Typhoon FLA 9500 GE Healthcare). Signals were analyzed with the ImageQuant TL software (Cytiva) and expressed as percentage of the pulse (t = 0) sample.

Viability Assays

Cell Titer-Glo (Promega) viability assays were performed in 96-well plate according to the manufacturer's instructions. The Cre-mediated depletion of Grp170 was induced by the addition of doxycycline (3 ug/ml) for the indicated number of days.

Indirect Immunofluorescence

E8 cells grown on glass coverslips were treated with doxycycline for the indicated time points or were left untreated. Cells were then rinsed once with PBS, fixed for 20 min in 3.7% formaldehyde, rinsed with PBS containing 10 mM glycine (PBS-G), and permeabilized with 0.5% Triton X-100 in PBS-G for 3 min at room temperature. After washing, nonspecific binding sites were blocked by incubation for 5 min in PBS-G containing 0.25% (wt/vol) albumin. Coverslips were incubated for 1 h with rabbit polyclonal anti-KDEL antibody (1:250 dilution; PA1-013; Thermofisher) to label the ER followed by washing in PBS-G. Cells were then incubated for 30 min with secondary antibody Alexa Fluor goat antirabbit 647 (1:500; A21245; Thermofisher). Following secondary antibody treatment, cells were washed extensively with PBS-G and mounted onto slides using Prolong Diamond Antifade Mountant with DAPI (P36962; Thermofisher). Confocal images were captured using a Nikon Eclimpse Ti2-E A1R inverted microscope outfitted with an oil immersion 100X objective (NA 1.45). Whole cell area was measured using the GFP signal and Nikon's NIS-Elements software (Nikon Instrument, Melville, NY). Data were entered into Prism software (GraphPad, La Jolla, CA) for graphing and statistical analysis consisting of a Student's *t* test of the treatment groups versus the untreated control. Asterisks represent $p < 0.0001$. The scale shown is 10 μm.

ACKNOWLEDGMENTS

This work was supported by National Institutes of Health (NIH) grant GM54068 (to L.M.H.) and the American Lebanese Syrian Associated Charities of St. Jude Children's Research Hospital, NIH grants DK117162 (to T.M.B), and GM131732 and DK137329 (to J.L.B.). We also acknowledge the Brodsky and Hendershot labs for advice, reagents, and/or valuable insights during the course of this study. We are additionally indebted to the Itzen lab for providing a number of reagents for the AMPylation blots that were unavailable in the US and for sending a detailed protocol for using the antibody along with a positive control. Finally, we are thankful to Drs. Rachael Wood and Richard Ashman for help with fluorescence analyses and cell sorting, to Joseph Chambers (University of Cambridge) for suggesting we examine BiP AMPylation, and to Marcus Valentine for help with the FISH assay.

REFERENCES

Adams BM, Oster ME, Hebert DN (2019). Protein quality control in the endoplasmic reticulum. Protein J 38, 317–329.

Amin-Wetzel N, Saunders RA, Kamphuis MJ, Rato C, Preissler S, Harding HP, Ron D (2017). A J-Protein cochaperone recruits BiP to monomerize IRE1 and repress the unfolded protein response. Cell 171, 1625–1637.

Anttonen AK, Mahjneh I, Hämäläinen RH, Lagier-Tourenne C, Kopra O, Waris L, Anttonen M, Joensuu T, Kalimo H, Paetau A, *et al.* (2005). The gene disrupted in Marinesco-Sjögren syndrome encodes SIL1, an HSPA5 cochaperone. Nat Genet 37, 1309–1311.

Appenzeller-Herzog C, Ellgaard L (2008). The human PDI family: versatility packed into a single fold. Biochim Biophys Acta 1783, 535–548.

Balchin D, Hayer-Hartl M, Hartl FU (2016). In vivo aspects of protein folding and quality control. Science 353, aac4354.

Behnke J, Hendershot LM (2014). The large hsp70 grp170 binds to unfolded protein substrates in vivo with a regulation distinct from conventional hsp70s. J Biol Chem 289, 2899–2907.

Behnke J, Feige MJ, Hendershot LM (2014). Mechanisms of action and biological functions of BiP's nucleotide exchange factors in the endoplasmic reticulum. J Mol Biol 427, 1589–1608.

Behnke J, Feige MJ, Hendershot LM (2015). BiP and its nucleotide exchange factors Grp170 and Sil1: Mechanisms of action and biological functions. J Mol Biol 427, 1589–1608.

Behnke J, Mann MJ, Scruggs FL, Feige MJ, Hendershot LM (2016). Members of the Hsp70 family recognize distinct types of sequences to execute ER quality control. Mol Cell 63, 739–752.

Bertolotti A, Zhang Y, Hendershot LM, Harding HP, Ron D (2000). Dynamic interaction of BiP and ER stress transducers in the unfolded-protein response. Nat Cell Biol 2, 326–332.

Blond-Elguindi S, Cwirla SE, Dower WJ, Lipshutz RJ, Sprang SR, Sambrook JF, Gething MJ (1993). Affinity panning of a library of peptides displayed on bacteriophages reveals the binding specificity of BiP. Cell 75, 717–728.

Bole DG, Hendershot LM, Kearney JF (1986). Posttranslational association of immunoglobulin heavy chain binding protein with nascent heavy chains in nonsecreting and secreting hybridomas. J Cell Biol 102, 1558–1566.

Braakman I, Bulleid NJ (2011). Protein folding and modification in the mammalian endoplasmic reticulum. Annu Rev Biochem 80, 71–99.

Brodsky JL, Werner ED, Dubas ME, Goeckeler JL, Kruse KB, McCracken AA (1999). The requirement for molecular chaperones during endoplasmic reticulum-associated protein degradation demonstrates that protein export and import are mechanistically distinct. J Biol Chem 274, 3453–3460.

Buck TM, Plavchak L, Roy A, Donnelly BF, Kashlan OB, Kleyman TR, Subramanya AR, Brodsky JL (2013). The Lhs1/GRP170 chaperones facilitate the endoplasmic reticulum-associated degradation of the epithelial sodium channel. J Biol Chem 288, 18366–18380.

Buck TM, Jordahl AS, Yates ME, Preston GM, Cook E, Kleyman TR, Brodsky JL (2017). Interactions between intersubunit transmembrane domains regulate the chaperone-dependent degradation of an oligomeric membrane protein. Biochem J 474, 357–376.

Chambers JE, Petrova K, Tomba G, Vendruscolo M, Ron D (2012). ADP ribosylation adapts an ER chaperone response to short-term fluctuations in unfolded protein load. J Cell Biol 198, 371–385.

Cheng MB, Zhang Y, Zhong X, Sutter B, Cao CY, Chen XS, Cheng XK, Zhang Y, Xiao L, Shen YF (2010). Stat1 mediates an autoregulation of hsp90beta gene in heat shock response. Cell Signal 22, 1206–1213.

Christianson JC, Jarosch E, Sommer T (2023). Mechanisms of substrate processing during ER-associated protein degradation. Nat Rev Mol Cell Biol.

Chung KT, Shen Y, Hendershot LM (2002). BAP, a mammalian BiP associated protein, is a nucleotide exchange factor that regulates the ATPase activity of BiP. J Biol Chem 277, 47557–47563.

Cowan NJ, Secher DS, Milstein C (1974). Intracellular immunoglobulin chain synthesis in nonsecreting variants of a mouse myeloma: detection of inactive light-chain messenger RNA. J Mol Biol 90, 691–701.

Craven RA, Egerton M, Stirling CJ (1996). A novel Hsp70 of the yeast ER lumen is required for the efficient translocation of a number of protein precursors. EMBO J 15, 2640–2650.

Cunningham CN, He K, Arunagiri A, Paton AW, Paton JC, Arvan P, Tsai B (2017). Chaperone-driven degradation of a misfolded proinsulin mutant in parallel with restoration of wild-type insulin secretion. Diabetes 66, 741–753.

Cunningham CN, Williams JM, Knupp J, Arunagiri A, Arvan P, Tsai B (2019). Cells deploy a two-pronged strategy to rectify misfolded proinsulin aggregates. Mol Cell 75, 442–456.e444.

Dancourt J, Barlowe C (2010). Protein sorting receptors in the early secretory pathway. Annu Rev Biochem 79, 777–802.

de Keyzer J, Steel GJ, Hale SJ, Humphries D, Stirling CJ (2009). Nucleotide binding by Lhs1p is essential for its nucleotide exchange activity and for function in vivo. J Biol Chem 284, 31564–31571.

Flynn GC, Pohl J, Flocco MT, Rothman JE (1991). Peptide-binding specificity of the molecular chaperone BiP. Nature 353, 726–730.

Fribley A, Zhang K, Kaufman RJ (2009). Regulation of apoptosis by the unfolded protein response. Methods Mol Biol 559, 191–204.

Gao G, Zhu C, Liu E, Nabi IR (2019). Reticulon and CLIMP-63 regulate nanodomain organization of peripheral ER tubules. PLoS Biol 17, e3000355.

Garcia VM, Nillegoda NB, Bukau B, Morano KA (2017). Substrate binding by the yeast Hsp110 nucleotide exchange factor and molecular chaperone Sse1 is not obligate for its biological activities. Mol Biol Cell 28, 2066–2075.
Gardner BM, Pincus D, Gotthardt K, Gallagher CM, Walter P (2013). Endoplasmic reticulum stress sensing in the unfolded protein response. Cold Spring Harb Perspect Biol 5, a013169.
Gülow K, Bienert D, Haas IG (2002). BiP is feed-back regulated by control of protein translation efficiency. J Cell Sci 115, 2443–2452.
Haapaniemi EM, Fogarty CL, Keskitalo S, Katayama S, Vihinen H, Ilander M, Mustjoki S, Krjutškov K, Lehto M, Hautala T, *et al*. (2017). Combined immunodeficiency and hypoglycemia associated with mutations in hypoxia upregulated 1. J Allergy Clin Immunol 139, 1391–1393.e1311.
Haas IG, Wabl M (1984). Immunoglobulin heavy chain toxicity in plasma cells is neutralized by fusion to pre-B cells. Proc Natl Acad Sci USA 81, 7185–7188.
Hao A, Wang Y, Zhang X, Li J, Li Y, Li D, Kulik G, Sui G (2021). Long non-coding antisense RNA HYOU1-AS is essential to human breast cancer development through competitive binding hnRNPA1 to promote HYOU1 expression. Biochim Biophys Acta Mol Cell Res 1868, 118951.
Harding HP, Zhang Y, Bertolotti A, Zeng H, Ron D (2000). Perk is essential for translational regulation and cell survival during the unfolded protein response. Mol Cell 5, 897–904.
Harding HP, Zhang Y, Scheuner D, Chen JJ, Kaufman RJ, Ron D (2009). Ppp1r15 gene knockout reveals an essential role for translation initiation factor 2 alpha (eIF2alpha) dephosphorylation in mammalian development. Proc Natl Acad Sci USA 106, 1832–1837.
Hendershot L, Bole D, Kohler G, Kearney JF (1987). Assembly and secretion of heavy chains that do not associate posttranslationally with immunoglobulin heavy chain-binding protein. J Cell Biol 104, 761–767.
Hendershot LM, Wei J-Y, Gaut JR, Lawson B, Freiden PJ, Murti KG (1995). In vivo expression of mammalian BiP ATPase mutants causes disruption of the endoplasmic reticulum. Mol Biol Cell 6, 283–296.
Hendershot LM, Buck TM, Brodsky JL (2023). The essential functions of molecular chaperones and folding enzymes in maintaining endoplasmic reticulum homeostasis. J Mol Biol 168418.
Hetz C, Zhang K, Kaufman RJ (2020). Mechanisms, regulation and functions of the unfolded protein response. Nat Rev Mol Cell Biol 21, 421–438.
Ichhaporia VP, Kim J, Kavdia K, Vogel P, Horner L, Frase S, Hendershot LM (2018). SIL1, the endoplasmic-reticulum-localized BiP co-chaperone, plays a crucial role in maintaining skeletal muscle proteostasis and physiology. Dis Model Mech 11, dmm033043.
Inoue T, Tsai B (2015). A nucleotide exchange factor promotes endoplasmic reticulum-to-cytosol membrane penetration of the nonenveloped virus simian virus 40. J Virol 89, 4069–4079.
Inoue T, Tsai B (2016). The Grp170 nucleotide exchange factor executes a key role during ERAD of cellular misfolded clients. Mol Biol Cell 27, 1650–1662.
Iurlaro R, Muñoz-Pinedo C (2016). Cell death induced by endoplasmic reticulum stress. Febs J 283, 2640–2652.
Kamijo T, Zindy F, Roussel MF, Quelle DE, Downing JR, Ashmun RA, Grosveld G, Sherr CJ (1997). Tumor suppression at the mouse INK4a locus mediated by the alternative reading frame product p19ARF. Cell 91, 649–659.
Kim DS, Song L, Wang J, Wu H, Gu G, Sugi Y, Li Z, Wang H (2018). GRP94 is an essential regulator of pancreatic β-Cell development, mass, and function in male mice. Endocrinology 159, 1062–1073.
Kitao Y, Ozawa K, Miyazaki M, Tamatani M, Kobayashi T, Yanagi H, Okabe M, Ikawa M, Yamashima T, Stern DM, *et al*. (2001). Expression of the endoplasmic reticulum molecular chaperone (ORP150) rescues hippocampal neurons from glutamate toxicity. J Clin Invest 108, 1439–1450.
Klopfenstein DR, Klumperman J, Lustig A, Kammerer RA, Oorschot V, Hauri HP (2001). Subdomain-specific localization of CLIMP-63 (p63) in the endoplasmic reticulum is mediated by its luminal alpha-helical segment. J Cell Biol 153, 1287–1300.
Kovacs P, Yang X, Permana PA, Bogardus C, Baier LJ (2002). Polymorphisms in the oxygen-regulated protein 150 gene (ORP150) are associated with insulin resistance in Pima Indians. Diabetes 51, 1618–1621.
Krshnan L, van de Weijer ML, Carvalho P (2022). Endoplasmic reticulum-associated protein degradation. Cold Spring Harb Perspect Biol 14, a041247.
Lee M, Song Y, Choi I, Lee SY, Kim S, Kim SH, Kim J, Seo HR (2021). Expression of HYOU1 via reciprocal crosstalk between NSCLC cells and HUVECs control cancer progression and chemoresistance in tumor spheroids. Mol Cells 44, 50–62.
Lievremont JP, Rizzuto R, Hendershot L, Meldolesi J (1997). BiP, a major chaperone protein of the endoplasmic reticulum lumen, plays a direct and important role in the storage of the rapidly exchanging pool of Ca2+. J Biol Chem 272, 30873–30879.
Lin HY, Masso-Welch P, Di YP, Cai JW, Shen JW, Subjeck JR (1993). The 170-kDa glucose-regulated stress protein is an endoplasmic reticulum protein that binds immunoglobulin. Mol Biol Cell 4, 1109–1119.
Luo S, Mao C, Lee B, Lee AS (2006). GRP78/BiP is required for cell proliferation and protecting the inner cell mass from apoptosis during early mouse embryonic development. Mol Cell Biol 26, 5688–5697.
Luo B, Lam BS, Lee SH, Wey S, Zhou H, Wang M, Chen SY, Adams GB, Lee AS (2011). The endoplasmic reticulum chaperone protein GRP94 is required for maintaining hematopoietic stem cell interactions with the adult bone marrow niche. PLoS One 6, e20364.
Molinari M, Hebert DN (2015). Glycoprotein maturation and quality control. Semin Cell Dev Biol 41, 70.
Munro S, Pelham HR (1987). A C-terminal signal prevents secretion of luminal ER proteins. Cell 48, 899–907.
Ng DT, Spear ED, Walter P (2000). The unfolded protein response regulates multiple aspects of secretory and membrane protein biogenesis and endoplasmic reticulum quality control. J Cell Biol 150, 77–88.
Park J, Easton DP, Chen X, MacDonald IJ, Wang XY, Subjeck JR (2003). The chaperoning properties of mouse grp170, a member of the third family of hsp70 related proteins. Biochemistry 42, 14893–14902.
Paton AW, Beddoe T, Thorpe CM, Whisstock JC, Wilce MC, Rossjohn J, Talbot UM, Paton JC (2006). AB5 subtilase cytotoxin inactivates the endoplasmic reticulum chaperone BiP. Nature 443, 548–552.
Perera LA, Ron D (2023). AMPylation and endoplasmic reticulum protein folding homeostasis. Cold Spring Harb Perspect Biol 15, a041265.
Phillips BP, Miller EA (2021). Membrane protein folding and quality control. Curr Opin Struct Biol 69, 50–54.
Pobre KFR, Poet GJ, Hendershot LM (2019). The endoplasmic reticulum (ER) chaperone BiP is a master regulator of ER functions: Getting by with a little help from ERdj friends. J Biol Chem 294, 2098–2108.
Poirier S, Mamarbachi M, Chen WT, Lee AS, Mayer G (2015). GRP94 regulates circulating cholesterol levels through blockade of PCSK9-induced LDLR degradation. Cell Rep 13, 2064–2071.
Porter AW, Nguyen DN, Clayton DR, Ruiz WG, Mutchler SM, Ray EC, Marciszyn AL, Nkashama LJ, Subramanya AR, Gingras S, *et al*. (2022). The molecular chaperone GRP170 protects against ER stress and acute kidney injury in mice. JCI Insight 7, e151869.
Qin JY, Zhang L, Clift KL, Hulur I, Xiang AP, Ren BZ, Lahn BT (2010). Systematic comparison of constitutive promoters and the doxycycline-inducible promoter. PLoS One 5, e10611.
Randow F, Seed B (2001). Endoplasmic reticulum chaperone gp96 is required for innate immunity but not cell viability. Nat Cell Biol 3, 891–896.
Ray FA, Peabody DS, Cooper JL, Cram LS, Kraemer PM (1990). SV40 T antigen alone drives karyotype instability that precedes neoplastic transformation of human diploid fibroblasts. J Cell Biochem 42, 13–31.
Robinson PJ, Bulleid NJ (2020). Mechanisms of disulfide bond formation in nascent polypeptides entering the secretory pathway. Cells 9, 1994.
Ron D, Walter P (2007). Signal integration in the endoplasmic reticulum unfolded protein response. Nat Rev Mol Cell Biol 8, 519–529.
Schiene-Fischer C (2015). Multidomain peptidyl prolyl cis/trans isomerases. Biochim Biophys Acta 1850, 2005–2016.
Schmidt BZ, Perlmutter DH (2005). Grp78, Grp94, and Grp170 interact with alpha1-antitrypsin mutants that are retained in the endoplasmic reticulum. Am J Physiol Gastrointest Liver Physiol 289, G444–455.
Senderek J, Krieger M, Stendel C, Bergmann C, Moser M, Breitbach-Faller N, Rudnik-Schoneborn S, Blaschek A, Wolf NI, Harting I, *et al*. (2005). Mutations in SIL1 cause Marinesco-Sjogren syndrome, a cerebellar ataxia with cataract and myopathy. Nat. Genet 37, 1312–1314.
Shen J, Chen X, Hendershot L, Prywes R (2002). ER stress regulation of ATF6 localization by dissociation of BiP/GRP78 binding and unmasking of Golgi localization signals. Dev Cell 3, 99–111.
Shibata Y, Shemesh T, Prinz WA, Palazzo AF, Kozlov MM, Rapoport TA (2010). Mechanisms determining the morphology of the peripheral ER. Cell 143, 774–788.
Skowronek MH, Hendershot LM, Haas IG (1998). The variable domain of nonassembled Ig light chains determines both their half-life and binding to BiP. Proc Natl Acad Sci USA 95, 1574–1578.
Steel GJ, Fullerton DM, Tyson JR, Stirling CJ (2004). Coordinated activation of Hsp70 chaperones. Science 303, 98–101.
Sukhoplyasova M, Keith AM, Perrault EM, Vorndran HE, Jordahl AS, Yates ME, Pastor A, Li Z, Freaney ML, Deshpande RA, *et al*. (2023). Lhs1

dependent ERAD is determined by transmembrane domain context. Biochem J 480, 1459–1473.
Tyson JR, Stirling CJ (2000). LHS1 and SIL1 provide a lumenal function that is essential for protein translocation into the endoplasmic reticulum. EMBO J 19, 6440–6452.
Vembar SS, Brodsky JL (2008). One step at a time: Endoplasmic reticulum-associated degradation. Nat Rev Mol Cell Biol 9, 944–957.
Walter P, Ron D (2011). The unfolded protein response: From stress pathway to homeostatic regulation. Science 334, 1081–1086.
Wanderling S, Simen BB, Ostrovsky O, Ahmed NT, Vogen SM, Gidalevitz T, Argon Y (2007). GRP94 is essential for mesoderm induction and muscle development because it regulates insulin-like growth factor secretion. Mol Biol Cell 18, 3764–3775.
Wang Y, Shen J, Arenzana N, Tirasophon W, Kaufman RJ, Prywes R (2000). Activation of ATF6 and an ATF6 DNA binding site by the ER stress response. J Biol Chem, 275, 27013–27020.
Wang J, Lee J, Liem D, Ping P (2017). HSPA5 Gene encoding Hsp70 chaperone BiP in the endoplasmic reticulum. Gene 618, 14–23.
Wang JM, Jiang JY, Zhang DL, Du X, Wu T, Du ZX (2021). HYOU1 facilitates proliferation, invasion, and glycolysis of papillary thyroid cancer via stabilizing LDHB mRNA. J Cell Mol Med 25, 4814–4825.
Wang W, Jiang X, Xia F, Chen X, Li G, Liu L, Xu Q, Zhu M, Chen C (2023). HYOU1 promotes cell proliferation, migration, and invasion via the PI3K/AKT/FOXO1 feedback loop in bladder cancer. Mol Biol Rep 50, 453–464.
Weitzmann A, Volkmer J, Zimmermann R (2006). The nucleotide exchange factor activity of Grp170 may explain the nonlethal phenotype of loss of Sil1 function in man and mouse. FEBS Lett 580, 5237–5240.
Williams JM, Inoue T, Chen G, Tsai B (2015). The nucleotide exchange factors Grp170 and Sil1 induce cholera toxin release from BiP to enable retrotranslocation. Mol Biol Cell 26, 2181–2189.
Wu X, Rapoport TA (2021). Translocation of proteins through a distorted lipid bilayer. Trends Cell Biol 31, 473–484.
Yamamoto K, Suzuki N, Wada T, Okada T, Yoshida H, Kaufman RJ, Mori K (2008). Human HRD1 promoter carries a functional unfolded protein response element to which XBP1 but not ATF6 directly binds. J Biochem 144, 477–486.
Yoshida H, Haze K, Yanagi H, Yura T, Mori K (1998). Identification of the cis-acting endoplasmic reticulum stress response element responsible for transcriptional induction of mammalian glucose-regulated proteins. Involvement of basic leucine zipper transcription factors. J Biol Chem 273, 33741–33749.
Zhao L, Longo-Guess C, Harris BS, Lee JW, Ackerman SL (2005). Protein accumulation and neurodegeneration in the woozy mutant mouse is caused by disruption of SIL1, a cochaperone of BiP. Nat Genet 37, 974–979.
Zhu G, Wang M, Spike B, Gray PC, Shen J, Lee SH, Chen SY, Lee AS (2014). Differential requirement of GRP94 and GRP78 in mammary gland development. Sci Rep 4, 5390.
Zinszner H, Kuroda M, Wang X, Batchvarova N, Lightfoot RT, Remotti H, Stevens JL, Ron D (1998). CHOP is implicated in programmed cell death in response to impaired function of the endoplasmic reticulum. Genes Dev 12, 982–995.
Zong ZH, Du ZX, Zhang HY, Li C, An MX, Li S, Yao HB, Wang HQ (2016). Involvement of Nrf2 in proteasome inhibition-mediated induction of ORP150 in thyroid cancer cells. Oncotarget 7, 3416–3426.